Chiang Mai J. Sci. 2016; 43(5) : 1160-1170
http://epg.science.cmu.ac.th/ejournal/
Contributed Paper

Effect of Nano-silica Addition on the Mechanical Properties and Thermal Conductivity of Cement Composites

Pongsak Jittabut [a], Supree Pinitsoontorn* [b], Prasit Thongbai [b], Vittaya Amornkitbamrung [b] and Prinya Chindaprasirt [c]

[a] Physics and General Science Program, Faculty of Science and Technology, Nakhon Ratchasima Rajabhat University, Nakhon Ratchasima, 30000, Thailand.

[b] Department of Physics, Faculty of Science, Khon Kaen University, Khon Kaen, 40002, Thailand.

[c] Sustainable Infrastructure Research and Development Center, Department of Civil Engineering, Faculty of Engineering, Khon Kaen University, Khon Kaen, 40002, Thailand.

*Author for correspondence; e-mail: psupree@kku.ac.th

Received: 29 July 2014
Accepted: 27 January 2015

ABSTRACT

This research article presents the mechanical properties and thermal conductivity of cement-based composite containing nano-silica. The effects of nano-silica particle size (12 nm, 50 nm and 150 nm) and concentration (1 - 5 wt.%) were systematically investigated. The compressive strength increases with certain amount of nano-silica due to the highly reactive nature of nano-silica which accelerates cement hydration reaction. Excessive nano-silica, on the other hand, leads to the decrease in strength since nano-silica absorb water required for cement hydration. This results in the creation of air void and lowers the bulk density. The maximum strength is obtained for the cement paste with 50 nm nano-silica of 4 wt.%. The compressive strength increases more than 50% in comparison to the control cement paste. For thermal conductivity measurement, adding nano-silica reduces thermal conductivity of the cement paste. The most effective agent for thermal resistivity is the 12 nm nano-silica due to the higher volume percent of air void formation. The thermal conductivity experimental results fit well with the theoretical models: the series model and the Maxwell's model.

Keywords: nanoparticles, cement composite, mechanical property, thermal conductivity, nano-silica, thermal conductivity model

1. INTRODUCTION

Nanoparticles have played an important role in improving properties of cement and concrete in recent years. The most widely used nanoparticle in cement related research is nano-silica [1-10] following the successful use of silica fume in cementitous products in the past [11, 12]. Nano-silica can improve the compressive strength of the cement paste [6, 9], mortar [1, 2] and concrete [3, 8] due to the filler effect of nano-size particles making

the denser products. Also, it can accelerate the cement hydration through the pozzolanic reaction to form C-S-H gel more quickly. Moreover, nano-silica can react with $Ca(OH)_2$ crystals to form C-S-H gel and even further strengthening the composite [1, 2, 4]. Qing et al. compared the effect of nano-silica and silica fume addition, and concluded that nano-silica can improve the mechanical properties much better than the silica fume case due to higher reactivity of nano-silica [6]. Givi et al. studied the size effects of nano-silica on the mechanical properties of binary blended concrete. They showed that the concrete with 15 nm silica particles have higher strength at the early age as compared to the concrete with 80 nm silica particles. This is due to the higher pozzolanic reaction for the smaller size [8]. However, nearly all related research have focused on mechanical properties, durability or workability of nano-silica cement composite but reports on other properties are rare.

Thermal conductivity of construction materials has received a lot of attentions since it is an important parameter related to energy conservation in buildings. Addition of many different materials on the thermal conductivity of cement-based materials has been reported, including cellulose and glass fibre, mineral wool, polystyrene, urethane foam and vermiculite [13-16]. Silica fume has also been introduced into cementitious materials in order to suppress thermal conductivity. It was shown that cement pastes mixed with silica fume exhibits >25% reduction of thermal conductivity in comparison to the plain cement paste [17, 18]. Nevertheless, there has not been any report on thermal conductivity of cement-based materials mixed with nano-silica. Thus, it would be of interest to investigate the effect of nano-silica addition on the thermal conductivity of the cement paste.

In this paper, we present the results on mechanical property and thermal conductivity of cement paste mixed with nano-silica. The concentration as well as the size of nano-silica was systematically investigated. The results were discussed based on cement hydration reaction and air void formation. The experimental results were fitted with thermal conductivity models.

2. MATERIALS AND METHODS

2.1 Sample Preparation

Ordinary Portland cement (OPC) conforming to the ASTM C150 standard was used. The chemical and physical properties of the cement are shown in Table 1. Three different sizes of nano-silica particles (the average diameter of 12, 50 and 150 nm) were used in this study. The properties of the utilized nano-particles are presented in Table 2.

Table 1. The chemical and physical properties of the Portland cement.

SiO_2 (%)	Al_2O_3 (%)	Fe_2O_3 (%)	CaO (%)	MgO (%)	K_2O (%)	Na_2O (%)	SO_3 (%)	Loss of ignition (%)	Specific surface area(m^2/g)
20.80	4.70	3.40	65.30	1.50	0.40	0.10	2.70	0.90	0.38

Table 2. Physical properties of the nano-silica obtained from manufacturers.

Nanoparticle	Purity (%)	Loss of ignition (%)	Specific surface area (m^2/g)
Nano-silica 12 nm	≥ 99.8	0.2	200
Nano-silica 50 nm	≥ 99.8	0.2	50
Nano-silica 150 nm	≥ 99.8	0.2	10

Three series of the nano-silica cement paste composite were prepared in this study. Series SA, SB and SC stand for the cement pastes with different nano-silica sizes of 12, 50 and 150 nm, respectively. In each series, the mixtures were prepared by substituting cement with nano-silica at 1-5 % by weight. The OPC paste was also prepared as a control sample. In order to obtain well dispersed nano-particles, prior to mixing with the cement, a small amount of water was added to the nano-silica powder and stirred at high speed (120 rpm) for 1 min. Subsequently, the wet nano-silica powder was added to the cement powder. The water to binder ratio (W/B) for all mixtures was fixed at 0.5 [1, 7, 10]. The cement - nano-silica pastes were mixed by a cement mixer for 3 min and were cast into 5cm×5cm×5cm moulds. The pastes were then compacted by tamping. After pouring into molds, an external vibrator was used to facilitate compaction and decrease the amount of air bubbles. The samples were demoulded after 24 h and then cured in air at room temperature and a relative humidity of 100% for 7 and 28 days. The mix proportions are presented in Table 3.

The workability of the paste was measured using the penetration test. The method was adapted from the consistency test of the paste using the Vicat needle (ASTMC187-11e1) [19]. The Vicat needle was 300 g in weight with a 10 mm diameter plunger. The penetrations of the plunger into the pastes were measured as an indicator of workability of cement paste.

Table 3. Mixture proportions of the pastes.

Mixture no.	Symbol	Size of nano-silica (nm)	OPC (g)	SA (g)	SB (g)	SC (g)	W/B	Water (g)
1	OPC	-	1,600	-	-	-	0.5	800
2	SA1	12	1,584	25	-	-	0.5	800
3	SA2	12	1,568	50	-	-	0.5	800
4	SA3	12	1,552	75	-	-	0.5	800
5	SA4	12	1,536	100	-	-	0.5	800
6	SA5	12	1,520	125	-	-	0.5	800
7	SB1	50	1,584	-	25	-	0.5	800
8	SB2	50	1,568	-	50	-	0.5	800
9	SB3	50	1,552	-	75	-	0.5	800
10	SB4	50	1,536	-	100	-	0.5	800
11	SB5	50	1,520	-	125	-	0.5	800
12	SC1	150	1,584	-	-	25	0.5	800
13	SC2	150	1,568	-	-	50	0.5	800
14	SC3	150	1,552	-	-	75	0.5	800
15	SC4	150	1,536	-	-	100	0.5	800
16	SC5	150	1,520	-	-	125	0.5	800

2.2 Characterization Techniques

The as-purchased nano-silica particles with the average diameter of 12, 50 and 150 nm were characterized by using an X-ray diffraction (XRD) technique (Bruker D8 Advance) with Cu-Ka radiation. After mixing, each paste was cured for 7 and 28 days and was subjected to the following tests. The morphology of the surface was investigated under the scanning electron microscope (SEM, JEOL-JSM-840A). The density of each sample was measured using an Archimedes method according to the ASTM B962-08 standard [20]. The percentage of air void was determined following the principle described in the ASTM3171-11 standard [21]. The compressive strength was tested in accordance with the ASTM C109 standard [22]. The strength value is an average of three measured data. The thermal conductivity of each paste was measured by a dynamic measurement method using the portable heat transfer analyzer (ISOMET 2114).

2.3 Thermal Conductivity Model

The thermal conductivity data obtain from the experiment was compared with thermal conductivity models. For simplicity, it is assumed that there are three components in the composite: the cement paste, the aggregate (nano-silica) and the air void. The thermal conductivity and density of each component are given in Table 4. Four thermal conductivity models were chosen for the comparison in this work.

Table 4. Thermal conductivity values of the different phases of cement paste.

Component	Thermal conductivity (W/m-K)	Density (kg/m^3)	Reference
Cement paste	1.019	1984	In this work
Nano-silica	1.38	2533	[23]
Air void	0.026	1.18	[24]

2.3.1 Series and parallel model

Mathematical expressions for the average thermal conductivity K for the series and parallel approximations are given in Eqs. (1) and (2). In the series arrangement, the poorest conductor of its component layer dominates the overall heat conduction. However, in the case of a parallel arrangement, the best conductor dominates the overall heat conduction [25].

$$\text{Series: } K = k_v\phi_v + k_c\phi_c + k_a\phi_a \quad (1)$$

$$\text{Parallel: } K = \frac{1}{\frac{\phi_v}{k_v} + \frac{\phi_c}{k_c} + \frac{\phi_a}{k_a}} \quad (2)$$

where K is the thermal conductivity of the composite, k_c is the thermal conductivity of the cement paste, k_a is the thermal conductivity of the aggregates (in this case nano-silica), k_v is the thermal conductivity of air, ϕ_v is the volume fraction of air voids, ϕ_c is the volume fraction of cement paste, and ϕ_a is the volume fraction of the nano-silica.

2.3.2 One-dimensional heat flow model

If the higher W/B ratios are used, the micro/nano pores may develop making the cement a better insulator. Taking this consideration into account, the one-dimensional heat flow model was proposed to predict the thermal conductivity of the cement composites as equation (3) [26]:

$$K = (\phi_a + \phi_c)\left[\frac{k_v k_c}{\phi_c k_v + \phi_v k_c} + (\phi_c k_c + \phi_a k_a)\right](1 - P_t) \quad (3)$$

where P_t is the total cement micro/nano porosity which is defined as

$$P_t = \frac{(W/B) - 0.17H}{0.317 + (W/B)} \quad (4)$$

and H represents the degree of hydration which is assumed to be unity for fully hydrated cement paste.

2.3.3 Maxwell's model

The Maxwell's model was extended by Brailsford and Major [27] for a wide range of dispersions. In this model, the constituent phases are mixed in a definite proportion for a two-phase system. This mixture is then embedded in a random mixture of the same two phase having conductivity equal to the average volume of the conductivity of phase system. Thus, the effective thermal conductivity of such a three-phase system can be determined as:

$$K = \left[\frac{k_c\phi_c + k_a\phi_a\left(\frac{3k_c}{2k_c + k_a}\right) + k_v\phi_v\left(\frac{3k_c}{2k_c + k_a}\right)}{\phi_c + \phi_a\left(\frac{3k_c}{2k_c + k_a}\right) + \phi_v\left(\frac{3k_c}{2k_c + k_a}\right)}\right] \quad (5)$$

3. RESULT AND DISCUSSION

3.1 Phase and Morphology

Figure 1 shows the XRD pattern of the as-purchased nano-silica particles. It can be seen that every pattern is similar. It shows a broad peak around 2θ of 22° which is the characteristic of amorphous silica. In general, the amorphous phase of silica is more reactive than the crystalline counterpart. Also, the higher surface area of the nanoparticles can increase the reaction rate. Thus, it is expected that the addition of nano-silica will influence the hydration reaction and the microstructure of the cement paste. The morphology of the surface of the cement pastes was studied under the SEM as shown in Figure 2. Figure 2 (a) shows the micrographs of the control cement paste cured for 28 days without an addition of nano-silica whereas the images in Figure 2(b) - (d) illustrates the surface of cement pastes with 4% nano-silica for the size of 12, 50 and 150 nm, respectively. From Figure 2(a), it was found that in the plain cement paste in the calcium silicate hydrate (C-S-H) gel existed in the form of the stand-alone clusters, and also lapped and jointed together by many needle-like hydrates. At the same time, deposited $Ca(OH)_2$ crystals were distributed among the cement paste [2]. On the other hand, an addition of nano-silica changed the microstructure of the cement paste shown in Figure 2(b)-(d). The texture of hydrate products was denser and more compact, and the sizes of $Ca(OH)_2$ crystal were also smaller than those of the control paste. This is probably due to the participation of nano-silica in the hydration process to generate C-S-H through the reaction with $Ca(OH)_2$.

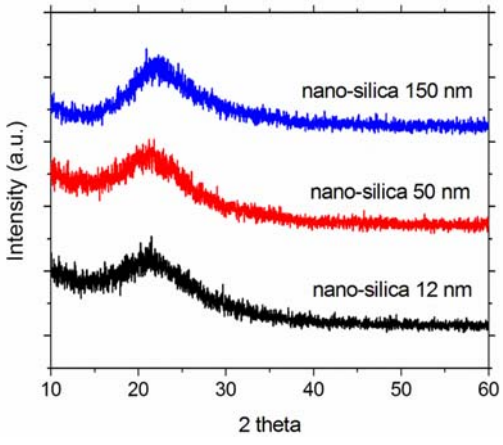

Figure 1. XRD pattern of nano-silica particle sizes of 12, 50 and 150 nm.

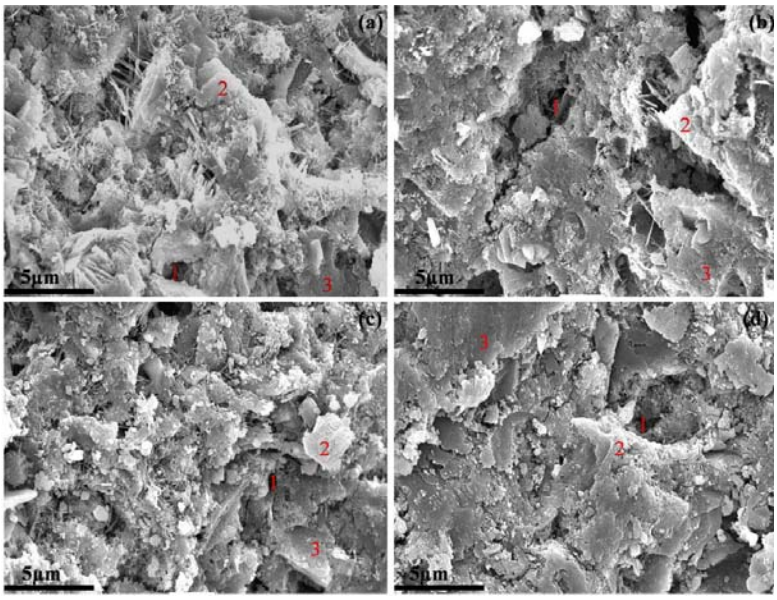

Figure 2. SEM micrographs of 4 wt% nano-silica - cement paste cured for 28 days with different nano-silica particle sizes: (a) without nano-silica, (b) 12 nm, (c) 50 nm, and (d) 150 nm. In the Figure, 1= pore, 2 = C-S-H, and 3= $Ca(OH)_2$.

3.2 Bulk Density of the Pastes

The variation of the paste density when adding nano-silica is shown in Figure 3. It can be clearly seen that for all nano-silica sizes, the addition of nano-silica reduced the sample density in comparison to the control cement paste. For the cement pastes with 12 nm nano-silica (Figure 3a), the density monotonously decreases with increasing amount of nano-silica. On the other hand, the cement pastes with 50 nm and 150 nm nano-silica (Figure 3b and 3c) showed a drop in density for the nano-silica addition of 1-2% and a slightly increase for 3-4% and a drop again at 5%. Overall, it can be concluded that the density has a tendency to decrease with an addition of nano-silica. This observation is different from the previous works [2, 10] where the increase in density was observed when nano-silica was added which was due to the filler effect of nano-silica. However, the earlier studies exploited the addition of superplasticizer in the mixture to control the flow rate. The superplasticizer can reduce the amount of water required in mixing the cement pastes but the amount of superplasticizer in each mixture is different. In the present study, we intend to investigate the effect of nano-silica addition on the mechanical and thermal properties without superplasticizer to control all other parameters under the same condition. As a result, with the same W/B ratios, the cement pastes become thicker for higher nano-silica concentration. This is because nano-silica has high surface area and can absorb water very quickly due to the hydration reaction of nano-silica. This interpretation is supported by the workability test as shown in Figure 3d where the penetration depth decreases for increasing amount of nano-silica. The replacement of cement with nano-silica resulted in the reduction in workability of the fresh pastes. Furthermore, the particle sizes had an effect on the workability of the

paste. The pastes with 12 nm nano-silica exhibited the lowest workability, followed by the pastes with 50 nm nano-silica and the pastes with 150 nm nano-silica. Thus, not all cement particles can react with water. This leads to the creation of small air void in the paste, and the amount of air void is related to the content of nano-silica as shown in Figure 3e. The nano-silica with 12 nm diameter has the highest surface area and therefore results in the more pronounced effect on the density than the 50 nm or 150 nm size.

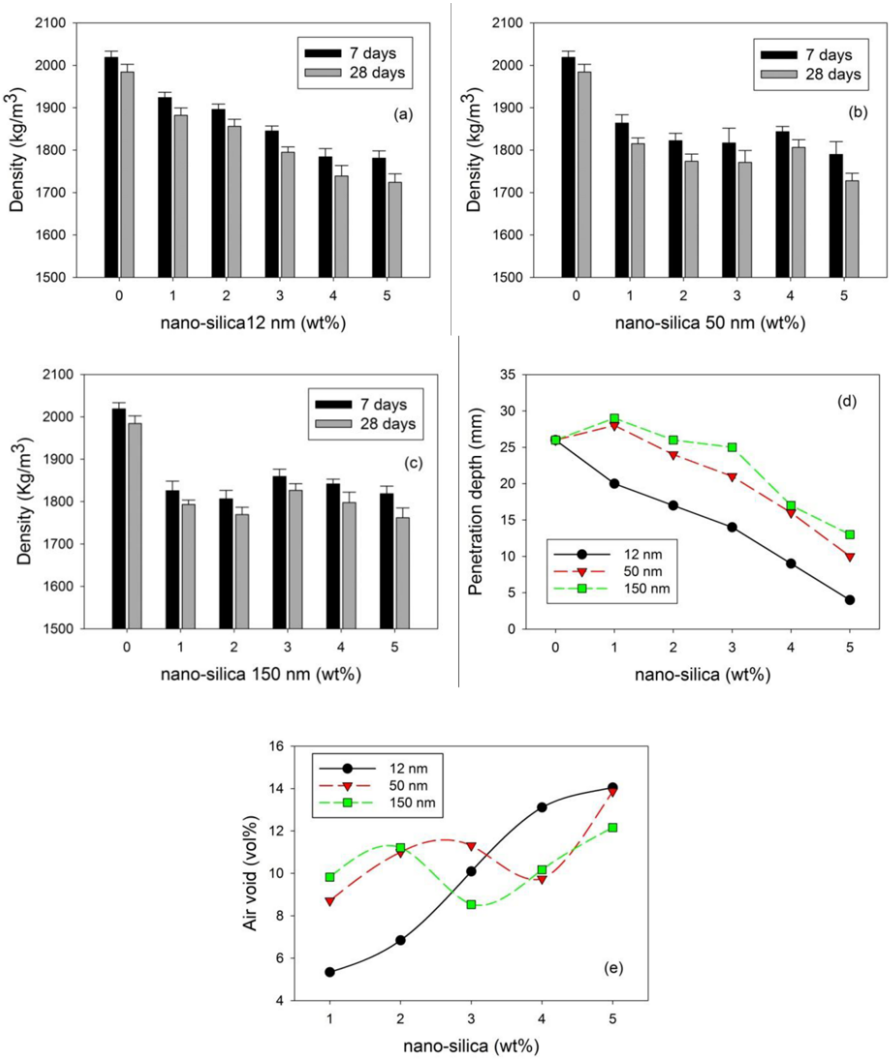

Figure 3. Bulk density of 7- and 28-days cement paste with addition of nano-silica (a) 12 nm, (b) 50 nm, (c) 150 nm. (d) workability of the cement paste by penetration test and (e) the relative volume percent of air void at 28 days.

3.3 Compressive Strength of Pastes

The results of compressive strengths of nano-silica added cement pastes are shown in Figure 4. In order to compare the effect of nano-silica sizes, we plot the strength of cement paste with 12, 50 and 150 nm nano-silica in the same plot and separate the measurement at the age of 7 days and 28 days in Figure 4a and 4b, respectively. There are many interesting points regarding this plot. Firstly, the compressive strength increases to the maximum point with the addition of certain amount of nano-silica and then drops when excessive nano-silica is introduced. For 12 nm nano-silica, the pastes show the maximum strength at 1% addition while for 50 and 150 nm sizes, the strength is maximized at 4% nano-silica. Secondly, the size of nano-silica has a significant effect on the strength. The cement paste with 50 nm nano-silica shows the higher strength than the others, with the maximum strength of >50% higher than the control cement paste. The possible reasons for this experimental result are discussed as follows. When nano-silica was added, it stimulated the hydration reaction of the cement particles and form C-S-H gel resulting in the higher compressive strength. Moreover, nano-silica has pozzolanic reaction with the $Ca(OH)_2$ crystals to form additional C-S-H phase. This prevents the $Ca(OH)_2$ crystals from growing and strengthens the pastes. However, the excessive nano-silica absorbed water required for the cement hydration process, reducing the final C-S-H product. The nano-silica particle may also surround cement particles making them inaccessible to water. Also, when the nano-silica is not well dispersed, as in the case for excessive nano-silica content, the aggregated nano-silica can create weak zone in form of voids and lowered the compressive strength. Since 12 nm nano-silica is the most reactive, it is required only 1% to obtain the maximum strength and more than that amount leads to the adverse effect. On the other hand, for less reactive nano-silica with the particles size of 50 and 150 nm, it requires about 4% for the maximum strength. Furthermore, the strength of cement paste is related to the density. Since the density of pastes with 12 nm nano-silica is lower than those with 50 and 150 nm for high nano-silica%, the strength of paste with 12 nm nano-silica also drops. In addition, for all samples regardless the particle size and concentration, the compressive strength is higher for the samples cured at 28 days due to the advance in hydration.

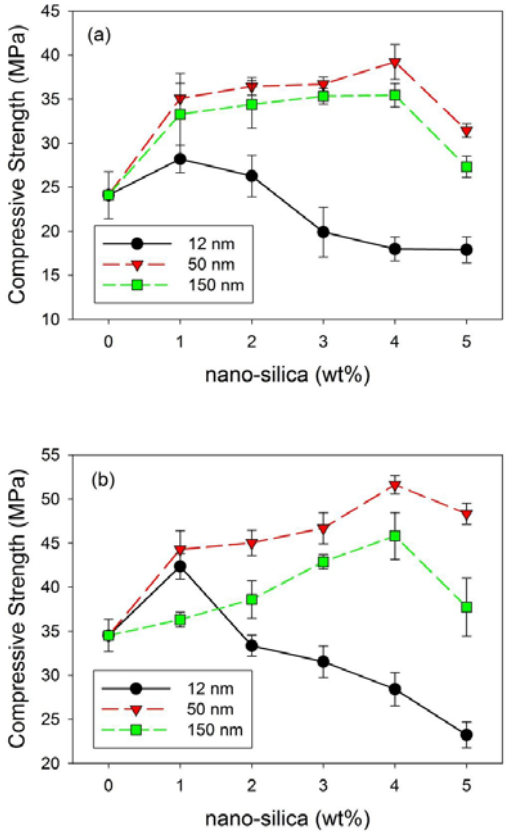

Figure 4. Compressive strength cement paste added nano-silica with different particle size, measured at (a) 7 days and (b) 28 days.

3.4 Thermal Conductivity of Pastes

The nano-silica - cement pastes of the size of 10cm × 10cm × 10cm were cured for 28 days before the thermal conductivity measurement. The results are shown in Figure 5. It can be obviously seen that the addition of nano-silica reduces the thermal conductivity monotonously. The most effective media to suppress thermal conductivity is when using the 12 nm particles. When reaching 5% of nano-silica, the thermal conductivity can be reduced by more than 20%. The main contribution of the reduction in thermal conductivity in the present study is due to the creation of small air void which suppress heat transfer significantly. The cement paste with 12 nm nano-silica contains highest air void and thus the effect is most pronounced. We can use the thermal conductivity model to fit the experimental data using the experimental values of the thermal conductivity and volume fraction of cement paste, nano-silica and air void. The models used are: 1) the series model, 2) the parallel model, 3) the one-dimensional heat flow (1D) model, and 4) Maxwell's model. The results are shown in Figure 6 (a)-(c). It can be clearly seen that the series model and the Maxwell's model fit the experimental values very well whereas the parallel model and the 1D model are significantly different from experiment.

The well fitting of the thermal conductivity values with the theoretical model indicate that the presence of air void is an important mechanism in decreasing thermal conductivity. Figure 7 plots the experimental values of thermal conductivity versus the volume percent of air void for all nano-silica sizes. It can be seen that the relation of the air void and the thermal conductivity is linear. The cement paste with 12 nm nano-silica shows the higher slope. Thus, it can be concluded the most effective media to reduce thermal conductivity is the addition of smallest nano-silica.

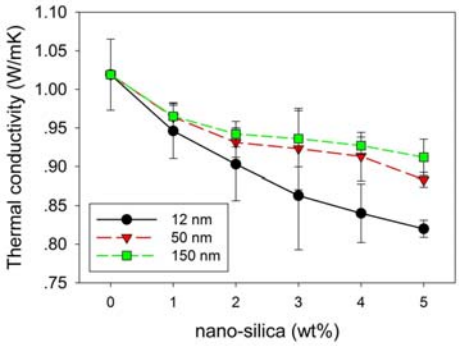

Figure 5. Thermal conductivity of nano-silica added cement paste.

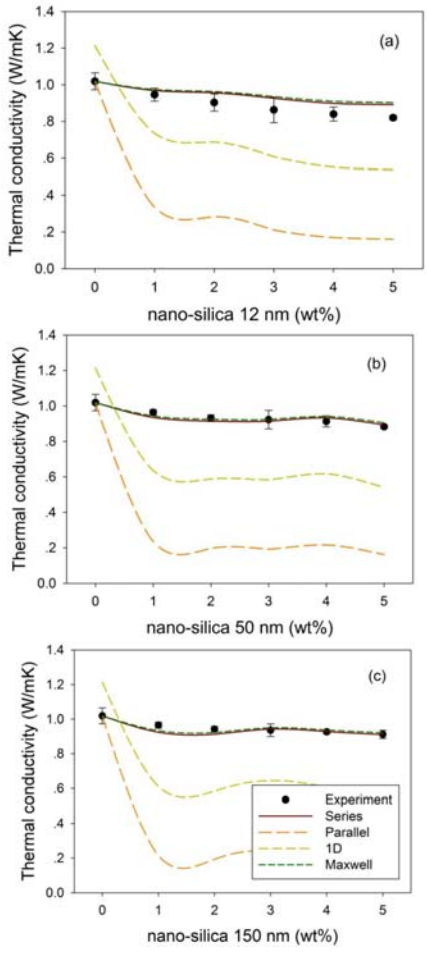

Figure 6. Comparison between experimental values and thermal conductivity models of cement paste with nano-silica (a) 12 nm, (b) 50, (c) 150 nm.

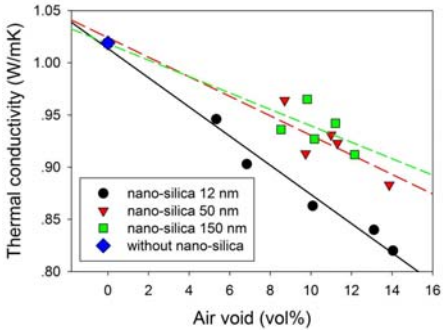

Figure 7. A plot of thermal conductivity of nano-silica added cement paste versus the volume percent of air void.

4. CONCLUSIONS

In this paper, the effects of the addition of nano-silica on both mechanical property and thermal conductivity of cement paste have been investigated. The compressive strength increases to the maximum values with the addition of certain amount of nano-silica due to the highly reactive nature of nano-silica which stimulates the hydration reaction. The 12 nm nano-silica particle with the largest surface area is the most reactive and can enhance the strength even with only 1 % by weight substitution. Higher content of nano-silica decreases the strength due to the lack of water for hydration reaction, the creation of weak zone from nonuniform distribution and the reduction of density. For thermal conductivity, addition of nano-silica can suppress thermal conductivity by means of air void formation. The thermal conductivity is most suppressed for cement paste with 12 nm nano-silica. Both series and Maxwell thermal conductivity models can fit the experimental results satisfactorily. For the use of nano-silica-cement composites for thermal insulation, it requires both strength and low thermal conductivity. Hence, the cement paste with 50 nm nano-silica of 4-5% is the most suitable composition which provides high compressive strength and relatively low thermal conductivity.

ACKNOWLEDGEMENTS

This work was supported by the Higher Education Research Promotion and National Research University Project of Thailand, Office of the Higher Education Commission, through the Advanced Functional Materials Cluster of Khon Kaen University, the Thailand Research Fund (TRF) and Khon Kaen University under the TRF Senior Research Scholar, Grant No. RTA5780004, and the Integrated Nanotechnology Research Center, Khon Kaen University.

REFERENCES

[1] Jo B.W., Kim C.H., Tae G.H. and Park J.B., *Constr. Build. Mater.,* 2007; **21**: 1351-1355. DOI 10.1016/j.conbuildmat. 2005.12. 020.

[2] Li H., Xiao H.G., Yuan J. and Ou J.P., *Compos. Part B-Eng.,* 2004; **35**: 185-189. DOI 10.1016/S1359-8368(03)00052-0.

[3] Nazari A. and Riahi S., *Compos Part B-Eng.,* 2011; **42**: 570-578. DOI 10.1016/j. compositesb.2010.09.025.

[4] Kawashima S., Hou P.K., Corr D.J. and Shah S.P., *Cement Concrete Comp.,* 2013; **36**: 8-15. DOI 10.1016/j.cemconcomp.2012. 06.012.

[5] Hou P.K., Kawashima S., Kong D.Y., Corr D.J., Qian J.S. and Shah S.P., *Compos. Part B-Eng.,* 2013; **45**: 440-448. DOI 10.1016/j.compositesb.2012.05.056.

[6] Qing Y., Zenan Z., Deyu K. and Rongshen C., *Constr. Build. Mater.,* 2007; **21**: 539-545. DOI 10.1016/j. conbuildmat.2005.09. 001.

[7] Senff L., Labrincha J.A., Ferreira V.M., Hotza D. and Repette W.L., *Constr. Build. Mater.,* 2009; **23**: 2487-2491. DOI 10. 1016/j.conbuildmat.2009.02. 005.

[8] Givi A.N., Rashid S.A., Aziz F.N.A. and Salleh M.A.M., *Compos. Part B-Eng.,* 2010; **41**: 673-677. DOI 10.1016/j.compositesb.2010.08.003.

[9] Stefanidou M. and Papayianni I., *Compos. Part B-Eng.,* 2012; **43**: 2706-2710. DOI 10. 1016/j.compositesb.2011.12.015.

[10] Berra M., Carassiti F., Mangialardi T., Paolini A.E. and Sebastiani M., *Constr. Build. Mater.,* 2012; **35**: 666-675. DOI 10.1016/j.conbuildmat.2012.04.132.

[11] Boddy A.M., Hooton R.D. and Thomas M.D.A., *Cem. Concr. Res.,* 2000; **30**: 1139-1150. DOI 10.1016/S0008-8846 (03)00100-5.

[12] Yajun J. and Cahyadi J.H., *Cem. Concr. Res.,* 2003; **33**: 1543-1548. DOI 10.1016/ S0008-8846 (00)00297-0.

[13] Zhou X.Y., Zheng F., Li H.G. and Lu C.L., *Energ Buildings,* 2010; **42**: 1070-1074. DOI 10.1016/j.enbuild.2010.01.020.

[14] Vrana T. and Bjork F., *Constr. Build. Mater.,* 2009; **23**: 1775-1787. DOI 10.1016/j.conbuildmat.2008.10.014.

[15] Mihlayanlar E., Dilmac S. and Guner A., *Mater. Design,* 2008; **29**: 344-352. DOI 10.1016/j.matdes.2007.01.032.

[16] Nicolajsen A., *Build. Environ.,* 2005; **40**: 907-914. DOI 10.1016/j.buildenv.2004.08.025.

[17] Fu X. and Chung D.D.L., *Cem. Concr. Res.,* 1997; **27**: 1799-1804. DOI 10.1023/A:1013889725971.

[18] Chung D.D.L., *J. Mater. Sci.,* 2002; **37**: 673-682. DOI 10.1016/S0008-8846(97)00174-9.

[19] ASTM. C187-98: Standard Test Method for Normal consistency of Hydraulic Cement. West Conshohocken, PA, USA: ASTM International; 2013.

[20] ASTM. B962 - 08: Standard Test Methods for Density of Compacted or Sintered Powder Metallurgy (PM) Products Using Archimedes' Principle. West Conshohocken, PA, USA: ASTM International; 2013.

[21] ASTM. D3171-11: Standard Test Methods for Constituent Content of Composite Materials. West Conshohocken, PA, USA: ASTM International; 2013.

[22] ASTM. C109 / C109M - 12: Standard Test Method for Compressive Strength of Hydraulic Cement Mortars (Using 2-in. or [50-mm] Cube Specimens). West Conshohocken, PA, USA: ASTM International; 2012.

[23] Wright A.F. and Lehmann M.S., *J. Solid State Chem.,* 1981; **36**: 371-380. DOI 10.1016/0022-4596(81)90449-7.

[24] Jirickova M., Pavlik Z., Fiala L. and Cerny R., *Int. J. Thermophys.,* 2006; **27**: 1214-1227. DOI 10.1007/s10765-006-0076-8.

[25] Carson J.K., Lovatt S.J., Tanner D.J. and Cleland A.C., *Int. J. Heat Mass Transfer,* 2005; **48**: 2150-2158. DOI 10.1016/j.ijheatmasstransfer.2004.12.032.

[26] Wong J.M., Glasser F.P. and Imbabi M.S., *Cement Concrete Comp.,* 2007; **29**: 647-655. DOI 10.1016/j.cemconcomp.2007.04.008.

[27] Brailsford A.D., Major K.G., *Br. J. Appl. Phys.,* 1964; **15**: 313-320.